

Thermomagnetic behaviour of haematite and goethite as a function of grain size in various non-saturating magnetic fields

Cor B. de Boer and Mark J. Dekkers

Paleomagnetic Laboratory 'Fort Hoofddijk', Utrecht University, Faculty of Earth Sciences, Budapestlaan 17, 3584 CD Utrecht, the Netherlands.
E-mail: cdeboer@geof.ruu.nl

Accepted 1997 November 11. Received 1997 November 3; in original form 1997 March 24

SUMMARY

When interpreting thermomagnetic curves of non-saturated magnetic minerals, irreversible heating and cooling curves need not necessarily imply chemical or structural changes. Increased aligning of magnetic moments on heating in an applied magnetic field can also induce an irreversible cooling curve. The two processes can be distinguished by stirring the sample between subsequent thermomagnetic runs. Sample redispersion considerably enhances the interpretative value of thermomagnetic analysis and is therefore strongly recommended, in particular when analysing non-saturated magnetic minerals.

Stirring between subsequent runs was extensively used in the analysis of the thermomagnetic behaviour of haematite and goethite as a function of grain size (i.e. coercivity) in various non-saturating magnetic fields (10–350 mT). The shape of the thermomagnetic heating curves of haematite is shown to be dependent on the competitive interplay between the temperature dependence of the exchange energy and that of the coercive force with respect to the applied field. On heating, pure defect-poor haematite, which is magnetically dominated by the canted moment, has an initially increasing thermomagnetic heating curve. Further heating causes the magnetization to increase smoothly up to a certain temperature which depends critically on the applied field and the coercivity of the sample. The irreversible block-shaped thermomagnetic cooling curve lies above the heating curve, and shows hardly any dependence on applied field and grain size. In contrast to the heating curve, the shape of the cooling curve depends only on the temperature variation of the exchange energy. Our data seem to indicate that for defect-poor haematites the domain configuration acquired at the maximum heating temperature is retained on cooling to room temperature. More defect-rich haematite has a gently decreasing thermomagnetic heating curve. On heating to increasingly elevated temperatures (800 °C) the defects are annealed out of the lattice, because the thermomagnetic curves approach those of defect-poor haematite. The defect moment due to lattice defects seems to be additive to, but softer than, the canted moment. The canted and defect moment appear to have the same Néel (or Curie) temperature (≈ 680 °C), because no change in temperature was observed, whilst the relative contributions did change. The thermomagnetic behaviour of goethite is shown to be dependent on its coercivity and the amount of substituted ions.

Key words: goethite, haematite, magnetization, rock magnetism.

1 INTRODUCTION

A Curie balance is a useful tool in magnetomineralogical research which is used to monitor the magnetization σ (σ_s when saturated) of a sample as a function of temperature. Thermomagnetic analysis not only provides mineral-specific Curie or Néel temperatures (T_C and T_N , respectively), but also

yields essential information concerning changes in magnetic structure and chemical reactions involving ferromagnetic minerals. For saturated ferromagnetic minerals, the heating and cooling curves of one complete thermomagnetic cycle are reversible if no chemical, structural or textural changes occur as a consequence of heating. The shape of the thermomagnetic curves depends in this case only on the temperature variation

of the exchange energy, which is a reversible process. Thermally induced chemical changes (e.g. dehydration, exsolution or, when measured in air, oxidation), structural changes (e.g. inversion, better ordering of the crystal lattice due to recrystallization or diffusion of lattice defects), and textural changes (e.g. sintering) may thus be detected by comparing the shape of heating and subsequent cooling curves.

The applied magnetic field in Curie balances, however, is often not sufficiently high to saturate hard magnetic minerals such as (ilmeno-)haematite, goethite, (oxidized) Ti-magnetites, some superficially oxidized greigites and fine-grained pyrrhotite. Consequently, in non-saturating fields the shape of the thermomagnetic curves also depends on the coercivity of the sample and its variation with temperature (Day 1975; Duff 1979). In this case, the irreversibility of the heating and subsequent cooling curve is not necessarily caused by chemical or structural changes of the mineral under investigation, but can also be caused by an irreversible magnetic 'aligning' process, as demonstrated by Day (1975) and Duff (1979) for synthetic titanomagnetite and natural haematite, respectively. Those observations, although acquired with rather insensitive Curie balances yielding noisy data, have received surprisingly little attention. Observed irreversible thermomagnetic behaviour is still often erroneously taken as evidence for thermally induced chemical or structural changes of non-saturated minerals.

Here, we present new data for two (synthetic and natural) submicron goethites and additional data for two natural haematites of different grain size, measured on a much more sensitive Curie balance (Mullender *et al.* 1993). It is shown that the shape of the thermomagnetic curves critically depends on the applied field and on the coercivity (i.e. grain size) of the sample. A pure, well-crystalline, 'defect-poor' haematite, which did not show any thermally induced chemical or structural changes, served as a reference for the measurement of field- and grain-size (i.e. coercivity) dependence of thermomagnetic curves. Deviations from this 'ideal' thermomagnetic behaviour are illustrated by the behaviour of a more 'defect-rich' haematite. For goethite, the difference between the thermomagnetic behaviour of a hard (synthetic) and a relatively soft (natural) sample is discussed. Redispersal of the sample followed by a repeated run to the same temperature is put forward as a tool for the detection of possible thermally induced chemical or structural changes.

2 RELEVANT ROCK MAGNETIC DATA

2.1 Haematite

Haematite (α -Fe₂O₃) is referred to as canted antiferromagnetic and has a saturation magnetization of $\approx 0.4 \text{ Am}^2 \text{ kg}^{-1}$ at room temperature (e.g. Stacey & Banerjee 1974; O'Reilly 1984). Reported σ_s -values vary between 0.2 and $0.5 \text{ Am}^2 \text{ kg}^{-1}$ (e.g. Néel & Pauthenet 1952; O'Reilly 1984). Above the Morin transition temperature ($T_M \sim -10^\circ\text{C}$) the antiferromagnetically coupled sublattice magnetizations lie in the basal plane orthogonal to the *c*-axis. A slight canting of the spin axis out of exact antiparallelism, however, results in a weak net ferromagnetic moment within the basal plane, perpendicular to the spin sublattices (Dzyaloshinsky 1958). In addition to this 'spin-canted moment', haematite may have a highly variable magnetization referred to as the 'defect moment'. Observed variations in σ_s are ascribed to this variable 'defect moment', which

is thought to arise from (an ordered structure of) lattice defects or from substituted non-magnetic cations (e.g. Néel 1953; Dunlop 1971; O'Reilly 1984). The 'defect moment' is therefore negligible in perfect, pure crystals and large in strained or otherwise imperfect grains. Because haematite is weakly magnetic only, one has to be aware that the measured properties of haematite samples are susceptible to the distorting effect of minute amounts of magnetic contaminants such as magnetite and maghemite.

At the Morin transition the spin orientation is changed from perpendicular to parallel to the *c*-axis. The antiferromagnetic coupling is retained but spin alignment is now perfect, that is canting has disappeared, resulting in no net magnetic moment. The 'defect moment', however, would not be affected by this spin reorientation and therefore remains below T_M . The temperature at which the Morin transition occurs, as well as its extent, are shown to be dependent on crystallinity and the amount of substitution in the haematite (e.g. Flanders & Remeika 1965; DeGrave *et al.* 1983). In pure haematite the Morin transition is completely suppressed in grains smaller than $\approx 0.03 \mu\text{m}$ (e.g. Bando *et al.* 1965; Schwertmann & Murad 1983). Dekkers & Linssen (1989) suggested that this grain-size limit may be larger for grains with sorbed silica and hydroxyl groups on their surfaces.

The Néel temperature of well-crystallized, pure haematite is generally reported to be $\approx 680^\circ\text{C}$. Substituted haematite has slightly lower values (e.g. Hutchings 1964). However, it is still debated whether or not the disappearance of the 'spin-canted moment' coincides with the antiferromagnetic T_N . Putnis (1992), for instance, reported that the spin canting vanishes around 675°C , but the antiferromagnetic coupling would persist up to $\approx 685^\circ\text{C}$. At higher temperatures the haematite is paramagnetic. This would imply that the 'defect moment' can be measured up to 685°C .

2.2 Goethite

Goethite (α -FeOOH) is antiferromagnetic but the spin compensation is imperfect, allowing a small net moment (e.g. Van Oosterhout 1965; Banerjee 1970; Hedley 1971). Sublattice magnetizations as well as the weak ferromagnetism of goethite lie along the crystallographic *c*-axis. Özdemir & Dunlop (1996) showed for well-crystallized, natural goethite that the ferromagnetic T_C coincides with the antiferromagnetic T_N at $120^\circ\text{C} \pm 2^\circ\text{C}$. However, reliable values between 70° and 130°C have been reported for T_N of goethite, depending on substitution, crystallinity, excess water and grain size (*cf.* Özdemir & Dunlop 1996 and references therein). Bocquet & Hill (1995), for instance, correlated reduced T_N values in fine-particle goethites with the concentration of iron vacancies, and proposed a cluster ordering model. Goethite can acquire a weak but very stable thermoremanent magnetization (TRM) with blocking temperatures up to 120°C (e.g. Strangway *et al.* 1967; Strangway *et al.* 1968; Banerjee 1970; Dekkers 1989a; Dekkers & Rochette 1992; Özdemir & Dunlop 1996). Observed saturation magnetizations are highly variable but are mostly in the range 10^{-2} to $10^{-1} \text{ Am}^2 \text{ kg}^{-1}$ (e.g. Bagin *et al.* 1976; Morris *et al.* 1985; Dekkers 1989b). Hedley (1971), however, reported σ_s -values increasing from 10^{-3} to $1 \text{ Am}^2 \text{ kg}^{-1}$ with rising aluminium content in the goethite.

2.3 Temperature dependence of the saturation magnetization

Haematites and goethites can show highly variable thermomagnetic behaviour. To explain observed differences between saturated and non-saturated behaviour and to distinguish different types of haematite and goethite by their thermomagnetic behaviour we need a reference σ_s - T curve typical of ideal crystals. In the case of haematite, calculated σ_s - T curves and curves based on thermal demagnetization of a TRM with high blocking temperatures of 'ideal' (pure and defect-poor) crystals are dispersed throughout the literature (e.g. Dunlop 1971; Pullaiah *et al.* 1975 and references therein). The reversible heating and cooling curves of saturated 'ideal' haematite are characterized by a typical block shape, with hardly any decrease in σ_s until $\approx 400^\circ\text{C}$ and a steep drop in magnetization after $\approx 650^\circ\text{C}$ to the Néel temperature. This characteristic shape indicates that for 'ideal' haematite, which is dominated by the canted moment, any decrease in exchange energy is almost negligible up to $\approx 400^\circ\text{C}$.

The σ_s - T curves measured by Rochette & Fillion (1989) can be taken as more or less 'model' σ_s - T behaviour for saturated, relatively pure, fine goethite crystallites. The thermomagnetic behaviour is characterized by an almost linear decrease in magnetization from $\approx 20\text{ K}$ to ≈ 10 – 20° below T_N . Above this temperature, the magnetization decreases more rapidly up to T_N .

3 SAMPLES AND METHODS

Two relatively pure natural haematite samples and two (synthetic and natural) goethite samples were used for the experiments. The haematite samples, labelled LH4 and LH6, are described by Hartstra (1982). The sized LH4 and LH6 fractions were crushed by Hartstra from massive pure haematite aggregates in a copper mortar and yielded platy and rounded grains, respectively. No significant substitution was detected by microprobe analyses. The lamellar texture of the LH6 haematite suggests that it is a completely martitized magnetite. Very few exsolution lamellae, probably of maghemite ($\gamma\text{-Fe}_2\text{O}_3$), were detected in the finest grain-size fraction under reflected light (*cf.* Hartstra 1982). Using alternating gradient magnetometer (MicroMag) measurements on fresh, non-heated material (Table 1), we found that apart from the finest fraction ($< 5\ \mu\text{m}$) of LH6 haematite, all grain-size fractions of LH4 haematite were also contaminated with a trace of a softer magnetic mineral. Consequently, data reported by Hartstra (1982) on these haematites are slightly biased by the magnetic contaminants. Test runs on the Curie balance indicated that the soft mineral in the LH6 sample was indeed maghemite (contribution to the signal $\leq 0.025\ \text{Am}^2\ \text{kg}^{-1}$ at room temperature, corresponding to ≈ 0.03 weight per cent), and that this spinel phase can easily be removed (i.e. inverted to haematite) by heating above $\approx 400^\circ\text{C}$, essentially without affecting the haematite (*cf.* Section 4.1.3; Fig. 2b). Therefore, we preheated the $< 5\ \mu\text{m}$ fraction to 700°C before measuring the field dependence of the thermomagnetic curves. The LH4 sample appeared to be contaminated with trace magnetite (contribution to the signal for the 30–40 μm fraction $\leq 0.05\ \text{Am}^2\ \text{kg}^{-1}$ at room temperature, corresponding to ≈ 0.05 weight per cent), which was, however, minimized (i.e. oxidized to haematite) to an insignificant amount after heating to 700°C in air (*cf.* Section 4.2).

The synthetic goethite sample is described by Dekkers &

Table 1. Hysteresis parameters of the haematite samples measured at room temperature with an alternating gradient magnetometer. The coarser grain-size fractions of both haematites reach almost saturation in the maximum applied field (1 T), while saturation did not occur for the $< 5\ \mu\text{m}$ fractions. Data of the fresh material is in some cases slightly biased by traces of a magnetically soft mineral (maghemite for the $< 5\ \mu\text{m}$ grain-size fraction of LH6 haematite, and magnetite for both fractions of LH4 haematite). Cycling to 800°C ($\approx 6^\circ\text{C}\ \text{min}^{-1}$) in an oven minimized the influence of these minerals. After this treatment the hysteresis loops were no longer slightly dented and wasp-waisted for the LH6 and LH4 haematite samples, respectively.

	H_c (mT)	H_{cr} (mT)	M_r/M_s
<i>LH6 fresh</i>			
55–75 μm	182 ± 4	204 ± 2	0.79 ± 0.03
$< 5\ \mu\text{m}$	279 ± 4	367 ± 1	0.74 ± 0.01
<i>LH6 800 $^\circ\text{C}$</i>			
55–75 μm	180 ± 3	197 ± 3	0.84 ± 0.03
$< 5\ \mu\text{m}$	324 ± 7	354 ± 1	0.92 ± 0.01
<i>LH4 fresh</i>			
55–75 μm	70 ± 4	129 ± 1	0.54 ± 0.05
$< 5\ \mu\text{m}$	100 ± 1	252 ± 1	0.57 ± 0.01
<i>LH4 800 $^\circ\text{C}$</i>			
55–75 μm	174 ± 4	244 ± 5	0.73 ± 0.02
$< 5\ \mu\text{m}$	277 ± 6	374 ± 5	0.76 ± 0.01

Rochette (1992). It was precipitated from an aqueous ferric nitrate solution at 30°C . The more or less rectangular grains (0.3–5 μm) have a granular texture with crystallite sizes ranging between 20 and 40 nm. The natural goethite was crushed from the massive outer rim of a rattle stone (museum piece). No concentric layering is visible in the sampled part. The sample contains a few per cent of intergranular silica and clay (J. J. van Loef, personal communication). The individual goethite crystallites of rattle stones are generally reported to be in the nanometer size range, and the goethite is slightly Al-substituted (van der Horst *et al.* 1994).

The $\sigma(T)$ curves for this study were measured in air with a modified horizontal translation Curie balance, which uses a cycling field instead of a steady field (Mullender *et al.* 1993). By cycling between the field values B_{\min} and B_{\max} the output signal is amenable to Fourier analysis. This makes continuous drift correction possible and the output signal can be processed further with a transversal filtering programme that considerably improves the signal-to-noise ratio. In this way the sensitivity has been increased by two to three orders of magnitude compared to conventional systems. Routine heating and cooling rates were $10^\circ\text{C}\ \text{min}^{-1}$ and 2 – $4^\circ\text{C}\ \text{min}^{-1}$ for the haematite and goethite samples, respectively. Typically, 50–100 mg samples of material were weighed in the sample holder of the Curie balance.

With this ultrasensitive Curie balance the shape dependence of the thermomagnetic curves for non-saturated 'ideal' haematite on the applied field and on grain size (55–75 μm and $< 5\ \mu\text{m}$ fraction) can be resolved accurately. The curves are measured at various non-saturating cycling fields ranging from 10 to 350 mT. Incremental runs to increasingly elevated temperatures up to T_N were measured to describe the magnetization process at temperatures lower than the T_N of the sample material. Sample redispersion between subsequent thermomagnetic runs was used to distinguish between genuine chemical and structural/textural changes of the sample on the one hand and field-induced changes in the magnetization on the other.

After a thermomagnetic cycle, the sample was either redispersed with a copper stick inside the sample holder or it was taken out of the holder, redispersed, reweighed and measured again under identical experimental conditions.

4 RESULTS AND DISCUSSION

4.1 Pure defect-poor haematite

4.1.1 Shape of the thermomagnetic heating curves

The thermomagnetic heating curves to 700 °C measured as a function of applied cycling field are shown in Figs 1(a) and (b) for the 55–75 µm and <5 µm grain-size fractions, respectively, of LH6 haematite. In non-saturating fields, the shape of the thermomagnetic heating curves is obviously not only dependent on the temperature variation of the exchange energy, but also depends on the magnitude of the applied field. By comparing the results shown in Figs 1(a) and (b), it appears that the effect of the field intensity on the shape of the heating curve, however, is also grain-size dependent.

For both grain-size fractions, the heating curves obtained show initially a gradual increase in magnetization with temperature, rather than having the block shape typical of saturated ‘ideal’ haematite (*cf.* Section 2.3). The initial increasing parts of the heating curves obtained in the lower applied cycling fields (<100–150 and <150–200 mT for the 55–75 and <5 µm grain-size fractions, respectively) have a more or less concave shape. With increasing field intensity the shape of the curves changes to convex. Once convex, the initial parts of the curves become increasingly horizontal, approaching the characteristic block shape typical of saturated ‘ideal’ haematite. From a specific temperature—referred to as the peak temperature, T_p , and indicated in Figs 1(a) and (b) with solid circles—the magnetization starts to decrease up to the Néel point. The heating curve obtained in the lowest applied cycling field (10–30 mT) shows, for both grain-size fractions, a pronounced, relatively narrow maximum in magnetization close to the Néel temperature. With increasing field intensity, however, the peak in magnetization becomes broader and less apparent, and the maximum shifts to lower temperatures.

The high quality of the thermomagnetic curves allows the plotting of measured σ versus B_{\max} of the applied cycling field to obtain the magnetization curve at any temperature between room temperature and 700 °C. The resulting magnetization curves for room temperature, 300° and 600 °C are shown in Fig. 1(c) for the 55–75 µm grain-size fraction, and in Fig. 1(d) for the <5 µm fraction. Above the Néel temperature (≈ 680 °C) haematite is a paramagnet. Consequently, the $\sigma_{700^\circ\text{C}}-B_{\max}$ curves obtained show the paramagnetic field dependence of haematite at this temperature, which is, as expected, linear with the field intensity and grain-size independent.

For both grain-size fractions, the starting points of the thermomagnetic heating curves are related to the field intensity (Figs 1a and b). In non-saturating fields more magnetic moments become aligned with the field as the field strength increases, resulting in a higher magnetization. The relation between the initial magnetization measured at room temperature ($\sigma_{i,\text{RT}}$) and B_{\max} of the applied cycling field is clearly seen in Figs 1(c) and (d) from the S-shaped $\sigma_{i,\text{RT}}-B_{\max}$ magnetization curves obtained. The $\sigma_{i,\text{RT}}$ values, however, appear to be higher for the 55–75 µm grains than for the <5 µm grains in the

same applied cycling field, illustrated by the steeper slope of the $\sigma_{i,\text{RT}}-B_{\max}$ curve for the coarse grains than for the fine grains. In the field range used, the difference becomes progressively larger with increasing field strength. The observed difference can be explained by the difference in coercivity between the grain-size fractions. Values of the coercive force (B_c) measured at room temperature with an alternating gradient magnetometer in fields up to 1 T are ≈ 180 and ≈ 280 mT for the 55–75 and <5 µm fractions, respectively.

On heating, however, the coercive force of the non-saturated haematite grains will decrease owing to the gain in thermal energy. Until saturation, a decreasing coercive force yields a magnetization increasingly aligned with the field. In non-saturating fields, the observed shape of the thermomagnetic heating curve thus results from the competitive interplay between the temperature dependence of the exchange energy and that of the coercive force. Consequently, in temperature intervals with an overall increasing magnetization, the decrease in coercivity with temperature outweighs the natural tendency of magnetization to decrease with temperature caused by the descending exchange energy. The overall initial increase in magnetization with temperature (Figs 1a and b) is also expressed by the steeper magnetization curves obtained for 300 °C compared to the $\sigma_{i,\text{RT}}-B_{\max}$ curves (Figs 1c and d). In haematite the microscopic coercivity is dominated by magneto-elastic effects. Contrary to the variation of the exchange energy with temperature (*cf.* Section 2.3), the temperature dependence of the coercivity of ‘ideal’ haematite is not well known, but seems to be grain-size dependent. Dunlop (1971), for instance, suggested $H_c(T) \propto \sigma_s^8(T)$ for fine haematite particles, while Flanders & Schuele (1964) reported $H_c(T) \propto \sigma_s^3(T)$ for a large single crystal of haematite.

The change in shape of the initial increasing part of the thermomagnetic heating curves from more or less concave to convex (Figs 1a and b) appears to be related to the inflection point of the S-shaped magnetization curves (Figs 1c and d). With increasing temperature this inflection point of the magnetization curve shifts to lower applied fields. Thus, during heating, the thermomagnetic curve obtained will have a concave shape as long as the applied field is lower than the field that coincides with this inflection point of the corresponding magnetization curve. Consequently, convex-shaped thermomagnetic heating curves of non-saturated haematite correspond to the convex top part of the magnetization curves. The difference between the concave and convex shapes of the thermomagnetic curves is more pronounced for the coarse grains because the magnetization curves obtained are steeper than those for fine grains.

Above the peak temperature (T_p) the decrease in exchange energy becomes the dominating parameter in determining the shape of the heating curve, actually causing the peak and the observed overall decrease in magnetization up to T_N . The sharp peak in magnetization observed in the lowest applied field may be interpreted as being a Hopkinson-like peak, while the broader and less pronounced peaks can be seen as its extension to higher applied fields (strictly speaking, only the peaking of the low-field susceptibility just before T_C or T_N is referred to as the Hopkinson effect; susceptibility goes to infinity at T_N). The T_p s show, for both grain-size fractions, a different but clearly negative correlation with the applied field (Figs 1a and b). The temperature shift of the magnetization peak with applied field is larger for the coarse grains than for

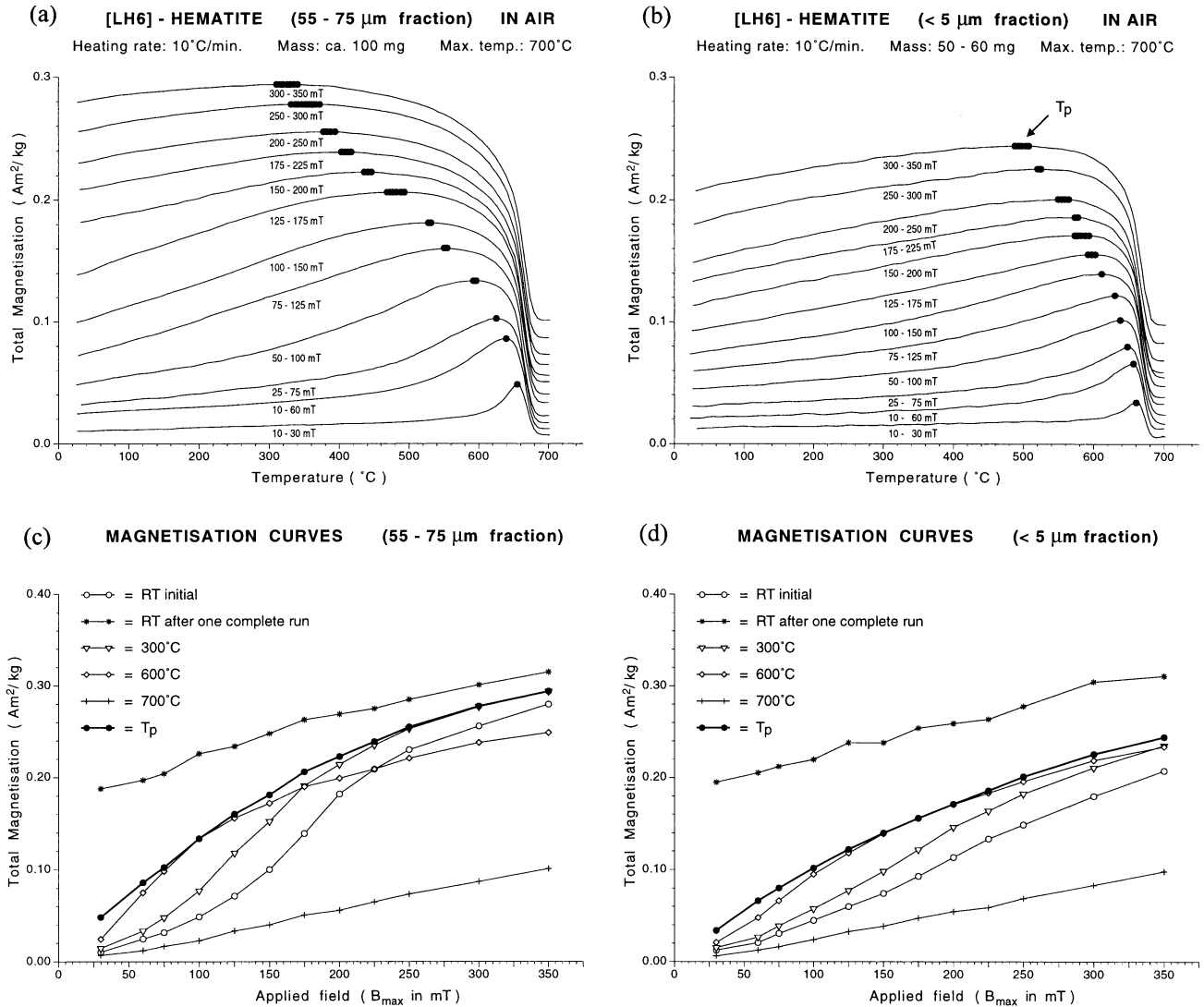


Figure 1. Thermomagnetic heating curves as a function of applied field for (a) the 55–75 μm and (b) the $< 5 \mu\text{m}$ grain-size fractions of pure ‘defect-poor’ LH6 haematite, measured in non-saturating cycling fields ranging from 10–350 mT. Comparison of both figures indicates that the shape of the heating curves critically depends on grain size (i.e. coercive force) if the applied fields are not sufficiently high to saturate the sample. Temperature variation of the coercive force is responsible for the initial increasing magnetization. Solid circles correspond to the temperature range in which the highest magnetization is reached. Above this temperature the shape of the heating curves is dominated by the temperature variation of the exchange energy. Temperature variation of the magnetization curves for (c) the 55–75 μm fraction and (d) the $< 5 \mu\text{m}$ fraction of LH6 haematite (room temperature: open circles; 300 °C: triangles; 600 °C: diamonds; 700 °C: pluses). Solid circles show the field dependence of the maximum magnetization values, and asterisks correspond to the field dependence of the magnetization measured at room temperature after a complete thermomagnetic cycle to 700 °C. The magnetization curves are derived from the thermomagnetic heating curves by plotting the measured magnetization versus B_{max} values of the applied cycling fields. We may use B_{max} values because the slopes of the asymmetric minor loops between B_{min} and B_{max} are very small, implying that the magnetic field actually acting can be equated to B_{max} (cf. Mullender *et al.* 1993). The field dependence of the magnetization measured at room temperature after a complete thermomagnetic cycle to 700 °C, together with the $\sigma_{i,\text{RT}}$, $\sigma_{300^\circ\text{C}}$ and T_p versus B_{max} curves, allows an estimate of the saturation magnetization of this haematite. As a consequence of the block shape and the irreversible thermomagnetic behaviour, these four curves will all coincide when the haematite sample is saturated. If we visually extrapolate them to higher field intensities the curves appear to coincide at a magnetization value between 0.35 and 0.4 $\text{Am}^2 \text{kg}^{-1}$. This estimated σ_s value agrees with literature values for pure ‘defect-poor’ haematite (cf. Section 2.1).

the fine grains. Apparently, in the field interval used, the shape of the heating curves depends more on the initial difference in coercivity between the grain-size fractions than on their different temperature variations of coercivity. In Figs 1(c) and (d) the T_p s are plotted against B_{max} of the applied cycling field. Both fractions show an approximately logarithmic increase of the magnetization peak value with applied field, which is larger for the coarse grains. We are not certain how exactly to

interpret this observed relation, but it clearly depends on the temperature variation of T_p which in turn is tied to the applied field and the coercivity of the sample.

4.1.2 Shape of the irreversible thermomagnetic cooling curves

The effect of the magnetic ‘aligning’ process on the shape of the thermomagnetic heating and subsequent cooling curve for

temperatures lower than the Néel temperature of haematite is shown in Fig. 2(a). Incremental runs to increasingly higher temperatures (maximum 700 °C) are measured for the 55–75 μm fraction of LH6 haematite in a 50–100 mT cycling field. As a consequence of the field adjustment procedure (see

Fig. 2c and its caption), the initial heating curve starts at a somewhat higher intensity than the corresponding curve in Fig. 1(a). Already at moderate temperatures the thermomagnetic heating and cooling curves are irreversible. Instead of initially showing a reversible, gradual decrease in

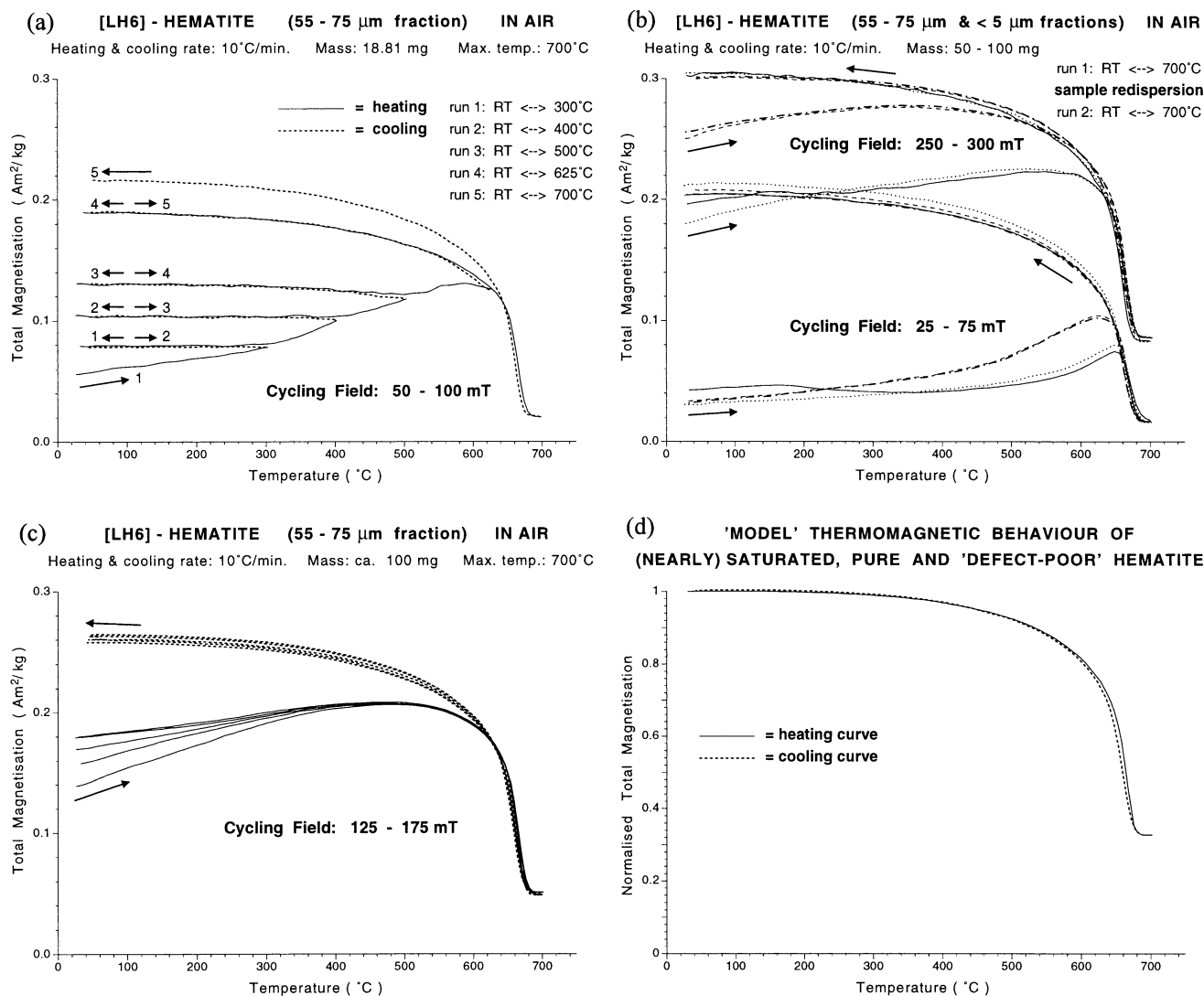


Figure 2. (a) Thermomagnetic behaviour for the 55–75 μm grain-size fraction of LH6 haematite in a 50–100 mT cycling magnetic field. Irreversibility between the heating curve and subsequent cooling curve is explained by field-induced changes in magnetization, rather than by thermally induced chemical or structural changes of the haematite. (b) Two subsequent thermomagnetic runs to 700 °C for the 55–75 μm fraction and < 5 μm fraction of LH6 haematite in a 25–75 mT and 250–300 mT cycling magnetic field. Run 1 is denoted by solid and dot-dashed lines, while run 2 is denoted by dotted and dashed lines for the < 5 and 55–75 μm grain-size fractions, respectively. Sample redispersion between the cycles is used to distinguish between chemical or structural changes of the haematite and field-induced changes of the magnetization. The fresh, non-heated, < 5 μm fraction of LH6 haematite appeared to be contaminated with a trace of maghemite, which, however, completely inverts to haematite upon heating above 400 °C. Apart from the removal of the trace maghemite, the thermomagnetic curves are fully recovered after sample redispersion, indicating that indeed only the magnetic ‘aligning’ process is responsible for the observed irreversible thermomagnetic behaviour. Cooling curves appear to be grain-size-independent and show only a slight field dependence. (c) Various initial thermomagnetic curves for the 55–75 μm grain-size fraction of LH6 haematite measured in a 125–175 mT cycling field. This shows a potential problem when dealing with non-saturated minerals. The observed differences between the curves are inherent in the field adjustment procedure of the Curie balance. A small (≤ 25 mT) but variable field overshoot is induced during the setting of the voltage. Apparently, the magnetization that became aligned during the field overshoot is retained in the desired field setting, which is (obviously) slightly lower. These variable starting points can be circumvented by setting the field range before suspending the sample in the measurement position. The heating curves coincide somewhere around 600 °C, but the maximum in magnetization is shifted to somewhat lower temperatures for higher initial magnetization values. The cooling curves, however, are identical within the measurement error. (d) Normalized thermomagnetic curves for the 55–75 μm grain-size fraction of LH6 haematite measured in a 300–350 mT non-saturating cycling field. The curves are obtained during a second run to 700 °C without sample redispersion in between. The thermomagnetic behaviour shown can be taken as representative for (nearly) saturated, pure and ‘defect-poor’ haematite, which is magnetically dominated by the canted moment. Note that the paramagnetic signal at 700 °C is about 33 per cent of the initial total magnetization signal.

magnetization, the magnetization reached on heating to temperatures up to $\approx 400^\circ\text{C}$ is retained on cooling to room temperature, resulting in almost horizontal cooling curves. The subsequent cooling curves start to diverge more and more from being horizontal until they approach the block shape typical of saturated 'ideal' haematite.

When dealing with 'ideal' haematite, the observed irreversibility between the heating and subsequent cooling curves indicates that the magnetic 'aligning' process becomes irreversible on cooling. On heating to, for instance, 300°C , the part of the magnetic moments that became aligned with the field due to the decrease in coercivity stays aligned with the field on cooling, producing the observed horizontal cooling curve. First, this implies that the shape of the cooling curves of non-saturated 'ideal' haematite is thus hardly influenced by the reversible temperature variation of the coercive force. Instead, it is dominated by the temperature variation of the exchange energy only, which appeared, however, to be negligible in the room temperature– 300°C temperature interval. Consequently, the observed cooling curve can be seen as equivalent to the horizontal low-temperature part of a block-shaped curve of saturated 'ideal' haematite. The difference between the heating and cooling parts can be seen as being the remanent part of the magnetization. The irreversible magnetic 'aligning' process is somewhat similar to the imparting of a partial TRM in a sample. Second, it apparently implies that for haematite the domain configuration at the maximum temperature (300°C in the example) is retained on cooling to room temperature, despite the decreasing thermal energy and the related increase in coercivity. Several authors (e.g. McClelland & Shcherbakov 1995; McClelland *et al.* 1996 and references therein) have published data relating to multiple changes in the domain structure of multidomain magnetites on cooling. Our observations indicate that this probably does not happen in haematite which is magnetically dominated by the canted moment. We realize that the domain state in the example is more likely to be single domain or few domain, so perhaps there are not many alternative local energy minima (LEM) states available. Grain-size fractions up to $250\text{--}425\ \mu\text{m}$, however, show similar behaviour.

On reheating to 400°C the cooling curve is reproduced until 300°C , because the maximum possible amount of aligned magnetic moments was already reached for that temperature in the applied field. Above 300°C , however, more magnetic moments become aligned with the field because of a further decrease in coercivity. The small divergence of the 500°C cooling curve from being horizontal indicates that at this temperature the change in exchange energy with temperature also becomes noticeable. After heating above T_N , the subsequent cooling curve approaches the block shape typical of saturated 'ideal' haematite. The part of the magnetic moments which stays aligned with the field during cooling from above T_N is a maximum for the field intensity used.

It appears that in the whole range of applied fields ($10\text{--}350\ \text{mT}$) the cooling curves are almost identical and all approach the characteristic block shape. Typical thermomagnetic runs to 700°C obtained in two different applied fields for the $55\text{--}75$ and $<5\ \mu\text{m}$ grain-size fractions are shown in Fig. 2(b). Contrary to the heating curves, the shape of the cooling curves shows hardly any dependence on the applied cycling field and grain size. The cooling curves are strongly dominated by the temperature dependence of the exchange

coupling, which in turn is almost independent of grain size and field strength. In the $T_N\text{--}600^\circ\text{C}$ interval, however, the curves obtained in the higher applied fields seem to be slightly steeper, that is they approach the block shape slightly more.

The magnetization values measured at room temperature after cooling from above T_N are plotted against B_{max} of the applied cycling fields ($10\text{--}350\ \text{mT}$) in Figs 1(c) and (d) for, respectively, the $55\text{--}75$ and $<5\ \mu\text{m}$ fractions. The parameters show a more or less linear relation, and the magnetization values obtained are almost the same for both grain-size fractions. Consequently, the maximum amount of magnetization which is retained in a certain field during cooling from above T_N is almost the same for both grain-size fractions, and thus more or less grain-size-independent in the interval used. This indicates that M_{rs}/M_s must also be almost identical for both grain-size fractions. This concurs with data from Dankers (1978, 1981) and Hartstra (1982), who reported that the isothermal saturation remanent magnetization is more or less grain-size-independent in a range from 250 to $5\ \mu\text{m}$ for LH6 haematite and some other natural haematite samples.

4.1.3 Sample redispersion

The observed irreversible thermomagnetic behaviour, however, might be erroneously taken as evidence for thermally induced chemical or structural changes of the haematite. Sample redispersion between subsequent cycles can be used to distinguish between these processes and field-induced changes in magnetization. If the observed irreversibility between the heating and cooling curves is caused only by the irreversible magnetic 'aligning' process, then the initial curves must be recovered after redispersion of the sample (Day 1975; Duff 1979). Fig. 2(b) shows two subsequent thermomagnetic cycles to 700°C for both grain-size fractions of LH6 haematite obtained in two different applied cycling fields ($25\text{--}75$ and $250\text{--}300\ \text{mT}$). After the first run to 700°C (which was performed on the fresh non-heated fractions) the sample was redispersed and remeasured under identical conditions. For the $55\text{--}75\ \mu\text{m}$ fraction, the initial curves are fully recovered after sample redispersion. This indicates that the haematite grains of this fraction were not affected chemically, structurally or texturally by the heating. The observed irreversibility between the heating and cooling curves of each individual cycle is thus only caused by the magnetic 'aligning' process.

The initial heating curves of the $<5\ \mu\text{m}$ fraction, however, are not fully recovered after sample redispersion. It is reasonable, however, to ascribe the observed difference to the maghemite contamination present in this fine-grained fraction (*cf.* Section 3). The difference in $\sigma_{i,\text{RT}}$ of $\approx 0.025\ \text{Am}^2\ \text{kg}^{-1}$ between the heating curves of the subsequent runs corresponds to a maghemite ($\sigma_s = 74\ \text{Am}^2\ \text{kg}^{-1}$) contamination of only ≈ 0.03 weight per cent. The marked drop in magnetization in the $180\text{--}350^\circ\text{C}$ interval during the first run (solid lines in Fig. 2b) indicates the crystallographic inversion of $\gamma\text{-Fe}_2\text{O}_3$ to $\alpha\text{-Fe}_2\text{O}_3$ (e.g. de Boer & Dekkers 1996). Above 350°C , however, the heating curves of runs 1 and 2 are almost reversible in both applied fields. This indicates that the inversion to haematite was complete and, moreover, that the haematite itself hardly changed due to the heating.

This redispersion experiment clearly illustrates that for non-saturated samples, irreversibility of heating and cooling curves of one complete thermomagnetic cycle does not automatically

imply chemical alteration or structural change; it can also be caused by an irreversible magnetic 'aligning' process. Sample redispersion between subsequent cycles is thus mandatory to distinguish between these two processes when applied fields are not sufficiently high to saturate the material.

4.1.4 Simulated 'model' behaviour of saturated 'ideal' haematite

Up to now we have compared the thermomagnetic behaviour of LH6 haematite with the calculated or otherwise derived model σ_s - T curve for 'ideal' haematite (cf. Section 2.3). LH6 haematite does not alter on heating to 700 °C, has an estimated σ_s close to reported values for pure 'defect-poor' haematite (cf. caption to Fig. 1), and moreover its thermomagnetic curves approach the block shape typical of 'ideal' haematite in the highest applied fields. Its thermomagnetic behaviour (cf. Figs 1 and 2) can be taken as representative of non-saturated pure and 'defect-poor' haematite, which is consequently dominated by the canted moment only.

Although the applied fields are not sufficiently high to saturate the sample, we can simulate saturated thermomagnetic behaviour by measuring two subsequent runs to 700 °C in the highest non-saturating fields without sample redispersion in between. After the first run to 700 °C the maximum magnetization is reached for the applied field. Consequently, the heating and cooling curves of the subsequent run are reversible and both have the typical block shape. As outlined in Section 4.1.2, the shapes of the cooling curves obtained in the applied non-saturating fields only show a slight field dependence. The curves of the second run thus give a justified estimate of the shape of the σ_s - T curve for this haematite. Fig. 2(d) shows the normalized curves of LH6 haematite (55–75 μm fraction) measured during a second run to 700 °C in a 300–350 mT cycling field without sample redispersion between the subsequent cycles. These measured curves have a similar shape to the calculated σ_s - T curves. These latter curves, however, apparently underestimate or do not take account of the paramagnetic contribution to the signal (≈ 33 per cent at 700 °C). Consequently, the measured curves shown in Fig. 2(d) better represent the 'model' σ_s - T curves for (nearly) saturated, pure defect-poor haematite.

4.2 Pure defect-rich haematite

We now present a natural haematite which shows a thermomagnetic behaviour noticeably different from the general trend outlined for 'ideal' LH6 haematite. The slightly contaminated LH4 haematite sample chemically and structurally changes upon heating. The haematite itself appears to be typical of a pure, more 'defect-rich' haematite, thus magnetically typified by a combination of the canted moment and the defect moment. Incremental thermomagnetic runs to increasingly higher temperatures for the 30–40 μm fraction of the platy LH4 haematite are shown in Fig. 3.

All curves show a distinct initial increase in magnetization up to ≈ 100 °C. This characteristic maximum in magnetization cannot have the same origin as the maximums observed in the thermomagnetic heating curves of non-saturated LH6 haematite because it is also visible in the subsequent cooling curves. Hartstra (1982) reported that the TRM and isothermal saturation remanence (referred to as I_{sr} by Hartstra) also peak at the same temperature (100 °C). He interpreted the initial

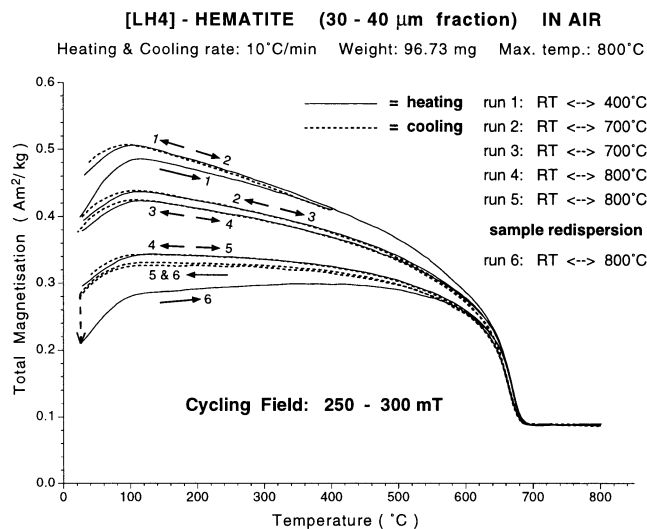


Figure 3. Thermomagnetic analysis of magnetite-contaminated 'defect-rich' LH4 haematite. On heating the magnetite is oxidized to haematite (run 2), and the defects are increasingly annealed out of the haematite lattice (runs 2 to 5), until a pure defect-poor haematite resides. Sample redispersion between runs 5 and 6 is denoted by the dashed arrow. The characteristic maximum in magnetization around 100 °C is caused only by the canted moment, and can most probably be seen as the onset of the Morin transition at this temperature.

increase in magnetization from room temperature to ≈ 100 °C as the onset of the Morin transition at this temperature, in contrast to commonly reported onsets of the Morin transition below room temperature (cf. Section 2.1). His low-temperature runs show that the decay in remanence (I_{sr} and TRM) takes place over a wide temperature interval starting at room temperature, rather than having an initial interval of hardly decreasing remanence. He suggested that the Morin transition for LH4 haematite was probably an interval (spanning a temperature range -75 °C to $+100$ °C), rather than a well-defined transition.

Apart from this remarkable initial increase, an overall decrease in magnetization with increasing temperature is observed, rather than the gradual initial increase in magnetization typical of non-saturated 'ideal' haematite. The initial magnetization at room temperature of LH4 haematite is significantly higher than the corresponding $\sigma_{i,RT}$ value of 'ideal' LH6 haematite measured in the same field. The first thermomagnetic cycle to 400 °C (run 1) causes an increase in magnetization on cooling; the cooling curve lies above the corresponding heating curve. Sample redispersion (not shown here) recovers the initial curves, implying that the observed irreversibility is caused only by the irreversible magnetic 'aligning' process. A subsequent run to 700 °C (run 2), however, results in a significant reduction of the magnetization. The cooling curve now lies below the corresponding heating curve. Sample redispersion (not shown here) no longer recovers the initial curves, indicating a thermally induced chemical and/or structural change of the haematite sample. Another run to 700 °C (run 3) causes only a small additional decrease in magnetization. Cycling to even higher temperatures (run 4, 800 °C), however, further reduces the magnetization. The cooling curve of this fourth run (Fig. 3) almost shows the block shape typical of pure 'defect-poor' haematite, apart from the onset of the Morin transition below 100 °C. A second run to 800 °C (run 5) reduces

the magnetization only slightly more and induces minute further changes in the block shape. Once obtaining this characteristic shape, no further changes in magnetization are observed upon repeated thermomagnetic runs to 800 °C (not shown here), and consequently the heating and cooling curves are now reversible. Sample redispersion (run 6, 800 °C) reduces the magnetization and results in an upward-convex heating curve with a maximum (T_p) at ≈ 360 °C. The irreversible cooling curve, however, has a block shape identical to that of run 5. The thermomagnetic behaviour of LH4 haematite now resembles the behaviour typical of a pure 'defect-poor' haematite.

Apparently, above 400 °C LH4 haematite starts to alter chemically and/or structurally to a pure 'defect-poor' haematite. MicroMag measurements detected a trace of a softer mineral in the grain-size fraction used (*cf.* Section 3). A hardly visible inflection between 550° and 600 °C in the heating curve of run 2 points to magnetite (Fe_3O_4 , $T_C = 580$ °C) as being the magnetic contaminant. The inflection point can hardly be seen in the field range used because it is obscured by the overall decrease in magnetization. The magnetite part, however, can be made more visible by applying much lower cycling fields (e.g. 10–60 mT, not shown here). This indeed revealed a clear inflection point around 580 °C, but more importantly it also showed that the trace magnetite ($\sigma_s = 92 \text{ Am}^2 \text{ kg}^{-1}$, contribution to the signal at room temperature $\leq 0.05 \text{ Am}^2 \text{ kg}^{-1}$ corresponding to ≤ 0.05 weight per cent) was completely oxidized to haematite during the two runs to 700 °C. Progressive oxidation of magnetite to haematite on heating is thus only partly responsible for the observed decrease in magnetization (runs 2–5); it cannot explain the irreversibility between the curves of run 3 and subsequent runs. Also, the magnetite contamination cannot account for the observed differences in magnetization between the curves in the 580–680 °C temperature interval.

After run 2, the measured magnetization at room temperature is still high compared to LH6 haematite, and the curves obtained do not resemble the thermomagnetic behaviour indicative of 'defect-poor' haematite (canted moment only). A defect magnetic moment superimposed on the canted moment is likely to be responsible for the relatively high initial magnetization. Several authors (e.g. Dunlop 1971, 1972; Bucur 1978) reported that the defect moment in particular is sensitive to heat treatment. The observed irreversible thermomagnetic behaviour may be explained by the presence of defects in the haematite lattice which are increasingly annealed out of the structure during heating. Heating to moderate temperatures (run 1, 400 °C) obviously does not significantly affect the defects present in the lattice (or the magnetite contamination). However, on heating to higher temperatures (700° and 800 °C), the defects are increasingly annealed out of the structure, that is heating diminishes the contribution of the defect moment to the signal. The magnetization decreases until the block shape typical of 'defect-poor' haematite remains. After sample redispersion (run 6) the slopes of the heating and cooling curves (apart from the first 100 °C) as well as the differences in magnetization between them are almost identical to LH6 haematite measured in the same field. LH4 haematite, however, still has a somewhat higher overall magnetization than the LH6 haematite. Because the haematites are now both magnetically dominated by the canted moment, we suggest that the

difference in absolute magnetization values is caused by a slightly different canting angle.

As mentioned before, the second run to 700 °C (run 3) is not biased any more by the trace amount of magnetite. The heating and cooling curves differ slightly, indicating that only a small additional amount of defects is annealed out of the haematite lattice. Consequently, the shape of these curves is not affected by the removal of the defects from the haematite lattice; the curves thus reflect the temperature variation of the canted and defect moment. By subtracting the contribution of the canted moment to the signal (block-shaped cooling curve of run 6) from the curves of run 3, we get an impression of the temperature variation of the magnetization caused by the defect moment only. The resulting thermomagnetic behaviour shows a gradual decrease in magnetization up to T_N . Apparently, the defect moment has its highest magnetization at room temperature, implying that this moment is saturated—or at least is close to saturation—in the applied field. Therefore, the defect moment due to lattice defects must be (much) softer than the canted moment. The temperature variation of the exchange energy apparently has a different effect on the defect moment than on the canted moment, because a convex-downward curve results instead of the block-shaped curve typical of the canted moment. The overall effect of a decreasing defect moment on heating is that the hardness of the haematite increases, as was demonstrated by Dunlop (1971, 1972) for SD haematite grains.

With the ultrasensitive Curie balance used, no shift of the inflection point near 680 °C to lower temperatures was observed upon continued cycling to 700° and 800 °C. This does not agree with earlier results (e.g. Aharoni *et al.* 1963; Smith & Fuller 1967), which suggested a difference between the temperature at which the spin canting vanishes (canted moment) and the temperature at which the antiferromagnetic coupling disappears (defect moment).

The characteristic maximum in magnetization around 100 °C is still present after repeated cycling and is thus caused only by the canted moment. Our findings support the earlier suggestion by Hartstra (1982) of an onset of the Morin transition at a relatively high temperature in this sample.

4.3 Goethite

4.3.1 Synthetic goethite

The thermomagnetic analysis (four incremental runs up to 100 °C) of a synthetic goethite is shown in Fig. 4(a). The fine goethite crystallites are reported to be pure (Dekkers & Rochette 1992). Therefore, the observed weakly ferromagnetic behaviour must have its origin in vacancies, crystal defects, excess structural OH^- or an odd number of spins, rather than in impurities. Heating this goethite sample to 40 °C (run 1) in a non-saturating cycling field (200–300 mT) results in an almost linear decrease in magnetization. The heating curve is reproduced on cooling. This thermomagnetic behaviour resembles the behaviour of the 'model' σ_s - T curve for goethite described in Section 2.3, suggesting that the shape of the curves, in the room temperature–40 °C temperature interval, is strongly dominated by the reversible temperature variation of the exchange energy. The start of a well-pronounced Hopkinson-like peak is observed on further heating (run 2, 60 °C). The heating-induced decrease in coercivity evidently

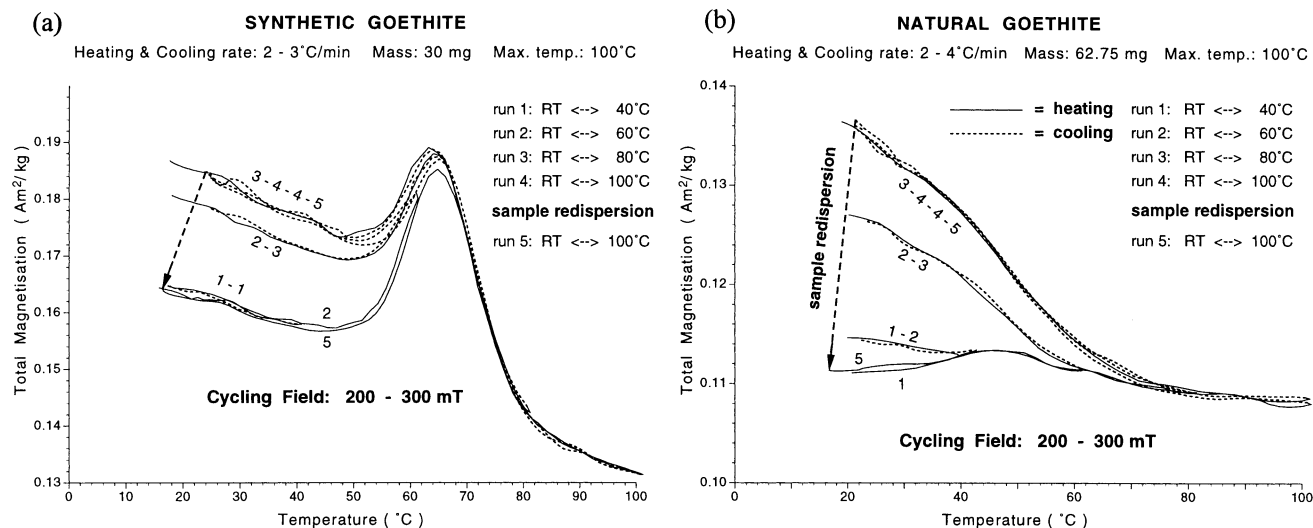


Figure 4. Thermomagnetic analysis of (a) a relatively hard synthetic goethite, and (b) a relatively soft, natural goethite.

becomes important above $\approx 50^\circ\text{C}$. Consequently, the magnetic moments can become increasingly aligned with the field, resulting in a sharp increase in magnetization. The heating and cooling curves of this second run are no longer reversible, implying that the magnetic 'aligning' process is also irreversible for goethite. However, on cooling from 60°C the magnetization first slightly decreases before it starts to increase at $\approx 50^\circ\text{C}$ according to the temperature variation of the exchange energy. The specific shape of the cooling curve indicates that, in the applied field, only part of the magnetic moments that became aligned with the field during heating to 60°C can stay aligned on cooling to room temperature. Heating to 80°C reveals the complete Hopkinson-like peak ($T_p \approx 65^\circ\text{C}$), and results in an additional increase in magnetization on cooling. The observation that the Hopkinson-like peak is partly preserved during cooling could imply the following two options: (1) some of the grains have very short relaxation times so that they essentially behave as superparamagnetic, or (2) the amount of acquired TRM (in the field of the Curie balance) is small compared to the height of the Hopkinson-like peak. In that case the peak will also be observable during the cooling run. A subsequent run to 100°C does not increase the magnetization; the heating and cooling curves are reversible. Consequently, the $T_c (= T_N)$ corresponding to the weak ferromagnetism must lie around 80°C . Sample redispersion (run 5, 100°C) recovers the initial heating curve, suggesting no major thermally induced chemical or structural changes in the goethite. Note that the T_p of $\approx 65^\circ\text{C}$ (Fig. 4a) corresponds to the maximum unblocking temperature of the CRM in Dekkers & Rochette (1992), while their measured maximum unblocking temperature of the TRM corresponds to the observed T_N of $\approx 80^\circ\text{C}$.

4.3.2 Natural goethite

When the natural goethite sample is subjected to identical experimental conditions (same incremental runs in the same applied cycling field) to the synthetic goethite, a slightly different thermomagnetic behaviour results (Fig. 4b). The weak ferromagnetism of this natural goethite is, in contrast to the pure synthetic goethite, most probably dominated by impurities. In particular, Al-substitution is commonly reported in

natural goethites (e.g. Fitzpatrick 1988; Van der Horst *et al.* 1994). Heating the natural goethite to 40°C (run 1) results in a small increase in magnetization, rather than in an initial decrease in magnetization as is observed for the non-saturated synthetic goethite. On cooling the thermomagnetic behaviour is irreversible. Consequently, the shapes of the thermomagnetic curves for this natural goethite sample are influenced by the decrease in coercivity from room temperature upwards. Knowing that both goethite samples have comparable grain-size ranges, this suggests that the natural goethite is relatively softer than the synthetic sample. The slightly lower total magnetization values of the natural goethite are explained by a small amount of clay and quartz contamination. Heating to higher temperatures (run 2, 60°C , and run 3, 80°C) allows more magnetic moments to become aligned with the field. On cooling, the magnetization increases to values far above the magnetization corresponding to the Hopkinson-like peak. The less pronounced Hopkinson-like peak and lower T_p ($\approx 46^\circ\text{C}$) of the natural goethite compared with the synthetic goethite support the supposed relative softness of this goethite. It could be that goethites which have their origin of the weak ferromagnetism predominantly in substituted cations are relatively softer than those with another origin. This agrees with data of Dekkers (1989a), who also mentioned that dispersed silica between individual goethite crystallites making up a grain may have a similar effect. Heating above 80°C (run 4, 100°C) does not result in any additional increase in magnetization on cooling, indicating that T_N is passed. The heating and cooling curves are now reversible and consequently approach the shape of saturated goethite (*cf.* Section 2.3). Redispersion of the sample recovers the initial heating curve, indicating that the goethite did not alter chemically during the thermal treatment. Despite the supposed different origin of the weak ferromagnetism and the different initial thermomagnetic behaviour, the heating-induced increase in magnetization (caused by the magnetic aligning process) for both goethites is almost the same ($\approx 0.025 \text{ Am}^2 \text{ kg}^{-1}$) after the complete experiment. Thus, on cooling from above T_N the same additional amount of magnetic moments is aligned with the field for both goethites, indicating that the remanence (specific 'TRM') for both goethites is similar.

5 CONCLUSIONS

The thermomagnetic behaviour of non-saturated minerals differs from that of saturated minerals in that it does not show reversible heating and cooling curves, in particular after heating above the T_N or T_C of the minerals. Apart from the temperature dependence of the exchange energy, the shape of the heating curve is shown to be dependent on the temperature variation of the coercivity with respect to the applied field. The cooling curves, however, show hardly any dependence on applied field and grain size (i.e. coercivity), and are dominated by the temperature dependence of the exchange energy. Thermomagnetic cycling thus results in a magnetization process if the applied field is not sufficiently high to saturate the sample. Consequently, in this case irreversible thermomagnetic behaviour does not automatically imply chemical or structural changes. Sample redispersion between subsequent runs is therefore mandatory to distinguish between field-induced changes on the one hand and chemical and/or structural changes on the other.

Initially increasing heating curves and block-shaped cooling curves appear to be indicative of non-saturated, pure and defect-poor haematite, which is magnetically dominated by the canted moment. The temperature which corresponds to the peak in magnetization observed on heating shows a negative correlation with the applied field. The temperature shift of the magnetization peak with applied field is larger for coarse grains than for fine grains due to the lower coercivity of the former. The domain configuration acquired at the maximum heating temperature is retained on cooling, suggesting that in multidomain defect-poor haematite no range of alternative local energy minima states is available.

Defects in the haematite lattice cause more gently decreasing heating curves. Annealing these more defect-rich haematites at increasingly elevated temperatures results in a thermomagnetic behaviour typical of defect-poor haematite. Our observations suggest that this particularly heat-sensitive defect moment is additive to the canted moment, and that it is distinctly softer than the canted moment. Furthermore, the temperature variation of the exchange energy seems to have a different effect on the defect moment due to lattice defects than on the canted moment. No difference is observed between the Néel temperature of the canted moment ($\approx 680^\circ\text{C}$) and the Curie point of the defect moment, as occasionally suggested in the literature.

The irreversible magnetic 'aligning' process acts on non-saturated goethite as well. The thermomagnetic behaviour of goethite is also shown to be dependent on coercivity.

ACKNOWLEDGMENTS

We thank Tom Mullender for helpful discussions and for keeping the Curie balance in top running condition. We acknowledge J. J. van Loef for providing the rattle stone. Two anonymous reviewers are thanked for helping to improve the original manuscript. This work was conducted under the programme of the Dutch national research school, the Vening Meinesz Research School of Geodynamics.

REFERENCES

Aharoni, A., Frei, E.H. & Schieber, M., 1963. Curie point and origin of weak ferromagnetism in hematite, *Phys. Rev.*, **131**, 1478–1482.

- Bagin, V.I., Gendler, T.S., Kuz'min, R.N., Rybak, R.S. & Urazayeva, T.K., 1976. The weak ferromagnetism of natural hydrogoethites, *Izv. Acad. Sci. USSR, Phys. Solid Earth, English translation*, **12**, 328–333.
- Bando, Y., Kiyama, M., Yamamoto, N., Takada, T., Shinjo, T. & Takaki, H., 1965. The magnetic properties of $\alpha\text{-Fe}_2\text{O}_3$ fine particles, *J. Phys. Soc. Japan*, **20**, 2086.
- Banerjee, S.K., 1970. Origin of thermoremanence in goethite, *Earth planet Sci. Lett.*, **8**, 197–201.
- Bocquet, S. & Hill, A.J., 1995. Correlation of Néel temperature and vacancy defects in fine-particle goethites, *Phys. Chem. Minerals*, **22**, 524–528.
- Bucur, I., 1978. Experimental study of the origin and properties of the defect moment in single domain hematite, *Geophys. J. R. astr. Soc.*, **55**, 589–604.
- Dankers, P.H.M., 1978. Magnetic properties of dispersed natural iron-oxides of known grain-size, *PhD thesis*, University of Utrecht.
- Dankers, P.H.M., 1981. Relationship between the median destructive field and remanent coercive forces for dispersed magnetite, titanomagnetite and hematite, *Geophysics J. R. astr. Soc.*, **64**, 447–461.
- Day, R., 1975. Some curious thermomagnetic curves and their interpretation, *Earth planet Sci. Lett.*, **27**, 95–100.
- De Boer, C.B. & Dekkers, M.J., 1996. Grain-size dependence of the rock magnetic properties for a natural maghemite, *Geophys. Res. Lett.*, **23**, 2815–2818.
- DeGrave, E., Chambaere, D.G. & Bowen, L.H., 1983. Nature of the Morin transition in Al-substituted hematite, *J. Magn. Magnetic Mater.*, **30**, 349–354.
- Dekkers, M.J., 1989a. Magnetic properties of natural goethite-I. Grain-size dependence of some low- and high-field related rockmagnetic parameters measured at room temperature, *Geophys. J.*, **97**, 323–340.
- Dekkers, M.J., 1989b. Magnetic properties of natural goethite-II. TRM behaviour during thermal and alternating field demagnetisation and low-temperature treatment, *Geophys. J.*, **97**, 341–355.
- Dekkers, M.J. & Linszen, J.H., 1989. Rock magnetic properties of fine-grained natural low-temperature haematite with reference to remanence acquisition mechanisms in red beds, *Geophys. J. Int.*, **99**, 1–18.
- Dekkers, M.J. & Rochette, P., 1992. Magnetic properties of chemical magnetisation in synthetic and natural goethite: prospects for a natural remanent magnetisation/thermoremanent magnetisation ratio paleomagnetic stability test? *J. geophys. Res.*, **97**, 17 291–17 307.
- Duff, B.A., 1979. Peaked thermomagnetic curves for hematite-bearing rocks and concentrates, *Phys. Earth planet. Inter.*, **19**, P1–P4.
- Dunlop, D.J., 1971. Magnetic properties of fine particle hematite, *Ann. Geophys.*, **27**, 269–293.
- Dunlop, D.J., 1972. Magnetic mineralogy of unheated and heated red sediments by coercivity spectrum analysis, *Geophys. J. R. astr. Soc.*, **27**, 37–55.
- Dzyaloshinski, I., 1958. A thermodynamic theory of 'weak' ferromagnetism of antiferromagnetics, *J. Phys. Chem. Solids*, **4**, 241–255.
- Fitzpatrick, R.W., 1988. Iron compounds as indicators of pedogenic processes: examples from the southern hemisphere, in *Iron in Soils and Clay Minerals*, pp. 351–396, eds Stucki, Goodman & Schwertmann, ASI Series Vol. C217, Riedel, Dordrecht.
- Flanders, P.J. & Remeika, J.P., 1965. Magnetic properties of hematite single crystals, *Phil. Mag.*, **11**, 1271–1288.
- Flanders, P.J. & Schuele, W.J., 1964. Temperature dependent magnetic properties of hematite single crystals, *Proc. Int. Conf. Magnetism*, Nottingham, 594–596.
- Hartstra, R.L., 1982. Some rockmagnetic parameters for natural iron-titanium oxides, *PhD thesis*, Utrecht University, Utrecht.
- Hedley, I.G., 1971. The weak ferromagnetism of goethite ($\alpha\text{-FeOOH}$), *Z. Geophys.*, **37**, 409–420.
- Hutchings, M.T., 1964. Point-charge calculations of energy levels of magnetic ions in crystalline electric fields, *Solid State Phys.*, **16**, 227–273.
- McClelland, E. & Shcherbakov, V.P., 1995. Metastability of domain

- state in multidomain magnetite: consequences for remanence acquisition, *J. Geophys. Res.*, **100**, 3841–3857.
- McClelland, E., Muxworthy, A.R. & Thomas, R.M., 1996. Magnetic properties of the stable fraction of remanence in large multidomain (MD) magnetite grains: single-domain or MD?, *Geophys. Res. Lett.*, **23**, 2831–2834.
- Morris, R.V., Lauer, H.V., Lawson, C.A., Gibson, E.K., Nace, G.A. & Stewart, C., 1985. Spectral and other physico-chemical properties of submicron powders of hematite (α -Fe₂O₃), maghemite (γ -Fe₂O₃), magnetite (Fe₃O₄), goethite (α -FeOOH) and lepidocrocite (γ -FeOOH), *J. Geophys. Res.*, **B90**, 3126–3144.
- Mullender, T.A.T., van Velzen, A.J. & Dekkers, M.J., 1993. Continuous drift correction and separate identification of ferrimagnetic and paramagnetic contribution in thermomagnetic runs, *Geophys. J. Int.*, **114**, 663–672.
- Néel, L., 1953. Some new results on antiferromagnetism and ferromagnetism, *Rev. Mod. Phys.*, **25**, 58–63.
- Néel, L. & Pauthenet, R., 1952. Etude thermomagnétique d'un monocristal de Fe₂O₃ α , *Compt. Rend.*, **234**, 2172.
- O'Reilly, W., 1984. *Rock and Mineral Magnetism*, Blackie, Glasgow.
- Özdemir, Ö. & Dunlop, D.J., 1996. Thermoremanence and Néel temperature of goethite, *Geophys. Res. Lett.*, **23**, 921–924.
- Pullaiah, G., Irving, E., Buchan, K.L. & Dunlop, D.J., 1975. Magnetisation changes caused by burial and uplift, *Earth planet. Sci. Lett.*, **28**, 133–143.
- Putnis, A., 1992. *Introduction to Mineral Sciences*, Cambridge University Press, Cambridge.
- Rochette, P. & Fillion, G., 1989. Field and temperature dependence of remanence in synthetic goethite: paleomagnetic implications, *Geophys. Res. Lett.*, **16**, 851–854.
- Schwertmann, U. & Murad, E., 1983. The effect of pH on the formation of goethite and hematite from ferrihydrate, *Clays Clay Mineral.*, **31**, 277–284.
- Smith, R.W. & Fuller, M., 1967. Alpha-hematite: stable remanence and memory, *Science*, **156**, 1130–1133.
- Stacey, F.D. & Banerjee, S.K., 1974. *The Physical Principles Of Rock Magnetism*, Elsevier, Amsterdam.
- Strangway, D.W., McMahon, B.E. & Honea, R.M., 1967. Stable magnetic remanence in antiferromagnetic goethite, *Science*, **158**, 785–787.
- Strangway, D.W., Honea, R.M., McMahon, B.E. & Larson, E.E., 1968. The magnetic properties of naturally occurring goethite, *Geophys. J. R. astr. Soc.*, **15**, 345–359.
- Van der Horst, A.A., van der Kraan, A.M., van Loef, J.J., Liefink, D.J. & Joosten, C., 1994. Mössbauer spectroscopic study of core and mantle of rattle stones, *Hyperfine Interactions*, **91**, 613–618.
- Van Oosterhout, G.W., 1965. The structure of goethite, *Proc. Int. Conf. Magnetism*, Nottingham (Institute of Physics, London), 529–532.